The use of UiO-type MOFs in vapour phase Soai reactions

Giuseppe Rotunno,[a,b] Gurpreet Kaur,[a,b] Andrea Lazzarini,[a,b] Carlo Buono,[a,b] Mohamed Amedjkouh [a,b] *

[a]Department of Chemistry, University of Oslo, P.O. Box 1033, Blindern, 0315 Oslo, Norway

[b]Center for Materials Science and Nanotechnology (SMN), Faculty of Mathematics and Natural Sciences, University of Oslo, P.O. Box 1126, Blindern, 0318 Oslo, Norway

E-Mail: mamou@kjemi.uio.no

Abstract

We report a novel vapour phase procedure to perform the Soai reaction in an absolute asymmetric synthesis fashion: the substrate is confined in the pores of the UiO-type MOFs, and vapour phase reactions with $Zn(i\text{-}Pr)_2$ are performed in a sealed environment, Different MOFs lead to different outcomes in terms of enantiomeric excess, handedness of the product and reaction rate. This is one of the first examples of absolute asymmetric synthesis performed inside a MOF.

Introduction

Chirality remains an intriguing scientific topic. Biomolecules in nature exhibit overwhelming one-handedness, often called homochirality, such as L-amino acids and D-sugars. The asymmetry can be introduced through a chiral auxiliary or a chiral catalyst.[1] Asymmetric catalysis can lead to the synthesis of enantiomerically pure chiral products in areas such as fine-chemicals and pharmaceuticals with growing need in the last decades.

In contrast with asymmetric catalysis, in which the structures of catalyst and product are different, in asymmetric autocatalysis a chiral product acts as chiral catalyst for its own production. [2] The Soai reaction remains a remarkable example of amplifying asymmetric autocatalysis.[3] [4] The addition of $Zn(i\text{-}Pr)_2$ to a rigid g-aminoaldehydes such as **1** in a toluene provides alkanols **2** with increasing ee. [5] Furthermore, it showed to be prone to amplification of ee despite the absence of the corresponding alcohol **2**, but in presence of various chiral factors [6] and, even more strikingly, in absence of any chiral substance.[7] Recently, asymmetric amplification of such autocatalysts was realized under heterogenous phase, *via* a heterogeneous vapour-solid interaction, by reaction of *iPr_2Zn vapor on achiral solid aldehyde*. [8][9] The synthesis of optically active compounds from achiral precursors has been defined as absolute asymmetric synthesis.[10]

In search for a validate mechanism of the remarkable asymmetric amplification efforts have been made using advanced techniques such as microcalorimetry [11], NMR analysis [12] and DFT calculations. [13] These analyses revealed the presence of dimers, tetramers and even higher-level aggregates in the reaction cycle. Combinatory studies of NMR and DFT techniques [14] [15] and XRD analysis of crystals [16] added support for these findings (Figure 1).

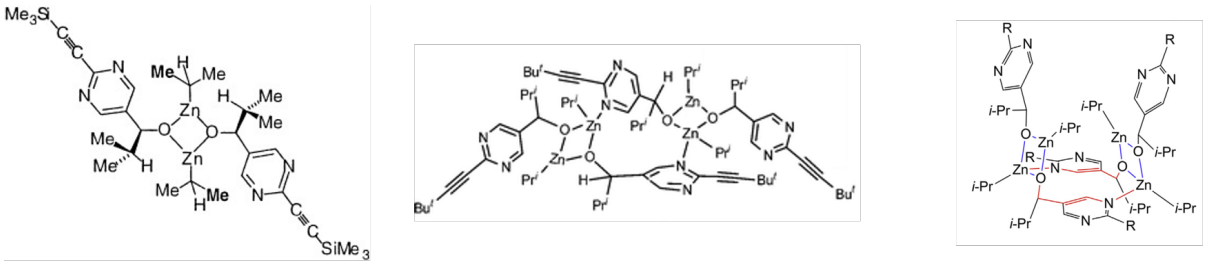

Figure 1. Selection of proposed or isolated reaction intermediates.

Gridnev *et al.* have computationally quantified the abundance of the species in the reaction pool [14]. Dimers were proposed as the resting state of the catalyst, while tetramers were found

as the active catalytic species. As proposed by Brown et al. [12c], once the reaction provides a tiny enantiomeric imbalance in the products, the *ee* can easily be propagated and amplified by the oligomerization of the reaction species. [17] Under homogeneous conditions, the dimers and tetramers involved in the reaction mechanism can diffuse in solution, associate and propagate in the three dimensions, and even grow into indefinite polymers. In a more recent investigations by Denmark *et al*. report on the function of the pyridyl- and pyrimidyl-moeity in the NMR studies revealing a tetrameric structure, also described as a cube escape model.[18]

Furthermore, the process is amenable to spontaneous molecular symmetry breaking under heterogeneous conditions by reaction of iPr_2Zn vapor-phase on solid aldehyde **1** [19]. Thus, in absence of solvent and with limited dynamic freedom the assembly and propagation of the reaction intermediates remains possible and allows for amplification in a constrained solid state.

A novel approach in the field is to mimic enzymes and perform asymmetric reactions in a pocket-like confined space. Metal-Organic Frameworks (MOFs) are porous crystalline materials, consisting of a 2D or 3D network [20]. Their framework consists of metal containing nodes known as secondary building units (SBUs) linked by multidentate organic ligands (linkers) by strong chemical bonds, that emerged as promising materials for various application such as catalysis, sensing, adsorption and separation due to their high porosity and large surface area and can be considered as nanoreactors.

MOFs provide an ideal platform for designing heterogenized asymmetric catalysts, by recreating the sophisticated interactions of an enzyme cavity, allowing for an efficient regio- and stereoselectivity. Moreover, unlike homogenous catalysts, well-defined active sites within the MOF framework are less prone to deactivation. In the last decade, researchers have applied a variety of synthetic strategies to build chiral MOFs for asymmetric catalysis and a large number of MOF-catalysed organic reactions have been reported [21].

Our interest focuses to probe confinement effects on the formation of the autocatalytic species and the extent of amplification if possible. MOFs provide an ideal platform for designing such heterogenized environment for the confinement of aldehyde molecules **1** in identical secondary environments inside the framework functioning as nanocontainers/reactors. Consequently, the oligomerization is subject to mesoporosity of the framework, which enforces limited propagation of the reaction intermediates through channel openings. To this end, it is imperative to probe MOFs with various open channels and linker functionalities because of the

need to transport typically very large organic substrates and products. This effect could significantly influence the final conversion and ee% of Soai alcohol **2** in the reaction.

As already stated, homochirality can arise spontaneously under absolute conditions in the Soai reaction on aldehyde **1**. Consequently, there was no need of a chiral MOF as asymmetric inductor/catalyst for our studies. The materials of our choice were UiO-type MOFs. UiO-66 and UiO-67 are formed by a metal cluster of 6 Zr(IV) ions arranged in an octahedron and, respectively, the organic linkers terephtalic acid (H_2bdc) and biphenyl-4,4'-dicarboxilic acid (H_2bpdc) *(Figure 2)*.

To the best of our knowledge, this is the first examples of absolute asymmetric autocatalysis performed into a MOF

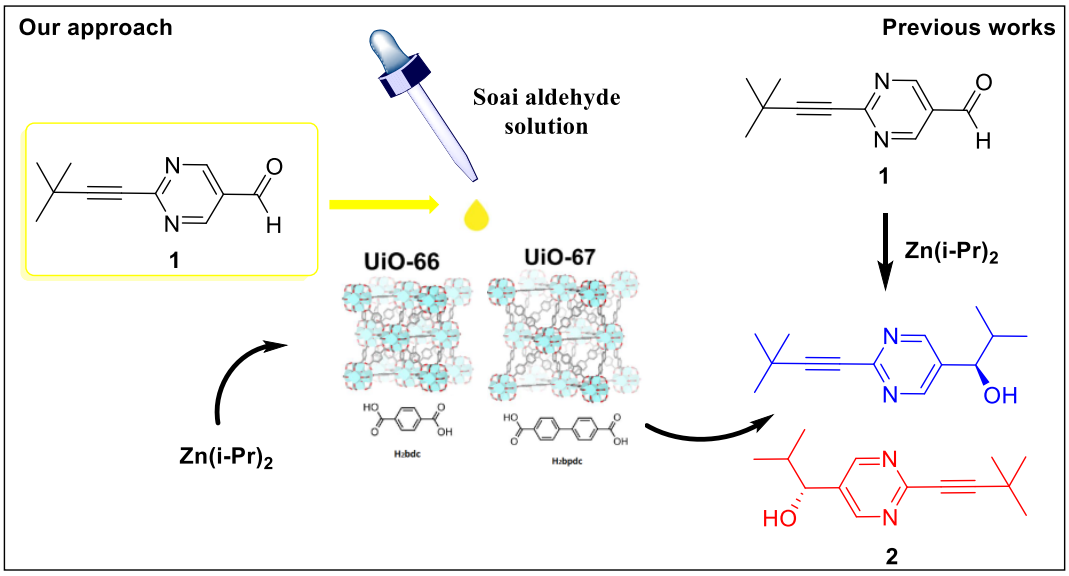

Figure 2. Concept of reactivity.

Inclusion

(a) Preliminary DFT calculations

Periodic DFT calculations have been performed in order to predict the position in which Soai aldehyde **1** would preferentially be allocated inside UiO-67 and UiO-66. Firstly, comparing the structures of **1** and the linkers of the two MOFs, the size of the aldehyde (10.5 Å) was found slightly smaller than the size of the biphenyl dicarboxylate linker of UiO-67, while terephtalic acid linkers of UiO-66 were almost half the size of the aldehyde. (See SI). The octahedral cages of the MOFs have been calculated being 16 Å for UiO-67 and 11 Å for UiO-66 [22].

In UiO-67, the optimized structure shows **1** physisorbed in the octahedral cage of the framework, with the formation of an H-bond between the hydrogen of the hydrated cornerstone of the MOF cluster and the oxygen of the carbonyl group of the aldehyde. In the UiO-66 the

cavity of the MOF is too small for the allocation of aldehyde **1** in the same position as in UiO-67. The most stable structure predicts the aldehyde inside the cavity establishing only weak van der Walls interactions with the organic linkers (Figure 3).

(b) The inclusion process

The inclusion of Soai aldehyde **1** has been performed by soaking sample of MOF powder in a toluene solution of **1**. The optimized ratio in weight between MOF and aldehyde was 1:2. The solution evaporated at r.t.: the slow evaporation of the solvent gradually concentrates the guest, which diffuses by capillary absorption and crystallizes inside the pores of the host. After complete evaporation, the MOF powder was washed and filtered under vacuum with acetone and oven-dried at 140 ºC.

The washing process is a key step that removes the excess of **1** present on the surface of the MOF, unbound to the framework. High Performace Liquid Chromatography (HPLC) analyses of the leakage of aldehyde **1** from an unwashed MOF sample showed the presence of **1** in solution already after few minutes. Samples analysed at later times indicated that the area of the aldehyde peak of **1** remained almost unchanged., due to the considerably higher amount of aldehyde **1** present on the surface and immediately released in solution compared to the amount leaked from the inside of the MOF. On the other hand, the concentration of **1** in a washed MOF sample slowly increased through time, proving a release and diffusion of the Soai aldehyde from the inside of the MOF to the solution with a significant reduction of the weakly coordinated aldehyde on the MOF surface *(Figure 4)*.

(c) Analyses on the MOF materials after inclusion of Soai aldehyde **1**

It was crucial to obtain a crystalline material after the inclusion step. In amorphous MOFs Soai aldehyde **1** would probably have been allocated in only certain areas of the MOF framework. Consequently, in such a MOF it is difficult to exploit the confinement effect and to evaluate the influence of the framework on the reactions. PXRD analysis of the MOF with included Soai aldehyde showed no loss in crystallinity compared to the starting material (See SI).

ATR-IR analysis (Attenuated Total Reflectance Infrared Spectroscopy) was performed on the materials. A series of diagnostic signals indicate the presence of aldehyde **1** in the framework of UiO-67 (red line of *Figure 5*). The signal at 1700 cm^{-1} can be attributed to the stretching of the carbonyl group of the Soai aldehyde **1**, furthermore the peak around 2200 cm^{-1} can be attributed to the C-N stretching of the aromatic ring while the C-H stretching of the terbutyl/isopropyl groups can be observed below 3000 cm^{-1}. Interestingly, the O-H stretching

of the hydroxyl groups of the clusters below 3700 cm^{-1} in the pristine material are perturbed in the UiO-67 after inclusion. This is a possible confirmation of the interaction with **1** predicted by the DFT calculations.

The ATR-IR analyses have also been performed on a sample of UiO-66 before and after the inclusion (*Figure 6*). The previously discussed signals of the aldehyde in the framework are present in UiO-66 after the inclusion treatment (blue line). Moreover, aldehyde **1** seems to be allocated in a different position in the framework of UiO-66 compared to UiO-67. This can be supported by the hydroxyl groups of the clusters not being perturbed in the sample after inclusion, meaning that the aldehyde is not interacting with them. Again, the results are in agreement with the DFT calculations.

(d) Quantification of the aldehyde in the different materials

In order to estimate the amount of aldehyde **1** included in the materials, two methods have been employed: leakage experiments followed by HPLC analysis and MOF digestion followed by NMR analysis. In the first method, the intensity of the absorption, and so the area of the aldehyde peak in the chromatogram, is proportional to its concentration in the liquid sample (Beer-Lambert law). However, it has been used only as an indirect method for a rough qualitative estimation, because the concentration will only represent the amount of aldehyde leaked from the MOF into the solution and not the amount present in the powder sample.

The second method is the MOF digestion by a media followed by NMR analyses of the resulting solution. The media dissolves the organic components of the MOF (linkers and aldehyde) while the inorganic portions precipitate as inorganic salts. NMR analysis allows to correlate the aldehyde signals with the signals coming from the linkers (*Figure 7*). This method can be considered a direct quantification of the amount of aldehyde in the material. With Zr-based MOFs, a basic digestion with NaOH in D_2O is normally employed. In our case, the Soai aldehyde **1** was found insoluble in the basic media. Instead, an acidic solution of 1% v/v D_3PO_4 in DMSO-d_6 was used as digestion media.

When analyses on the same materials have been made with the two methods, they have shown similar trends in the amount of aldehyde included (*Figure 8*). For instance, the inclusion process has been performed in MOFs with different linkers: pristine UiO-67, UiO-67 $bpy_{10\%}$, UiO-67 binaphtyl and UiO-66 (See SI). UiO-67 $bpy_{10\%}$ was the UiO-MOF in which the highest amount of aldehyde **1** was allocated. On the other hand, UiO-66 was the one with the lowest amount of guest inclusion. Interestingly UiO-67 binaphtyl, characterized by a much-hindered cage, was found able to allocate a slightly higher amount of Soai aldehyde compared to UiO-

67. This could be explained by π-π interactions between the naphtyl rings of the linker and the pyrimidine rings of aldehyde **1**.

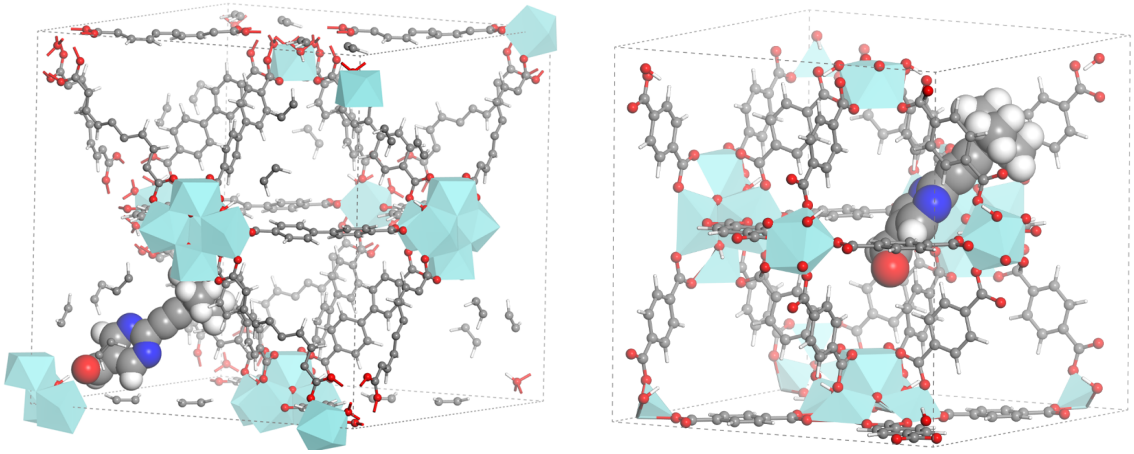

Figure 3. Periodic DFT calculations of **1** inside UiO-67 (left) and UiO-66 (right).

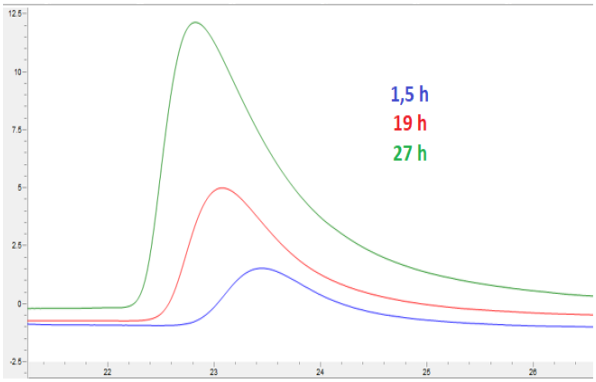

Figure 4. Leakage experiments from washed UiO-67.

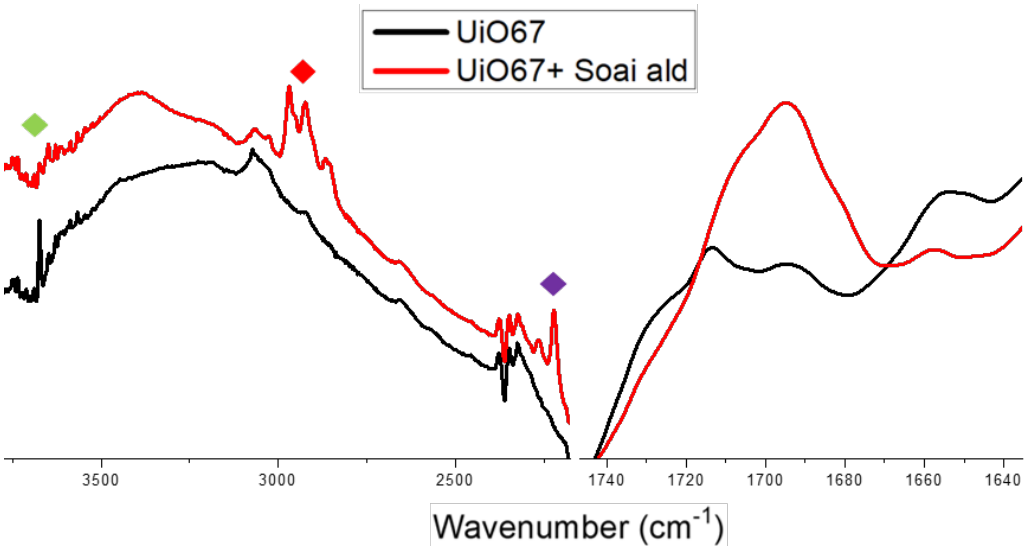

Figure 5. ATR-IR of UiO-67 and UiO-67 after inclusion of aldehyde 1. On the left, stretching of the hydroxyl groups (in green), stretching of the terbutyl/isopropyl groups (in red), stretching of the C-N of the ring (in purple). On the right, stretching of the carbonyl group.

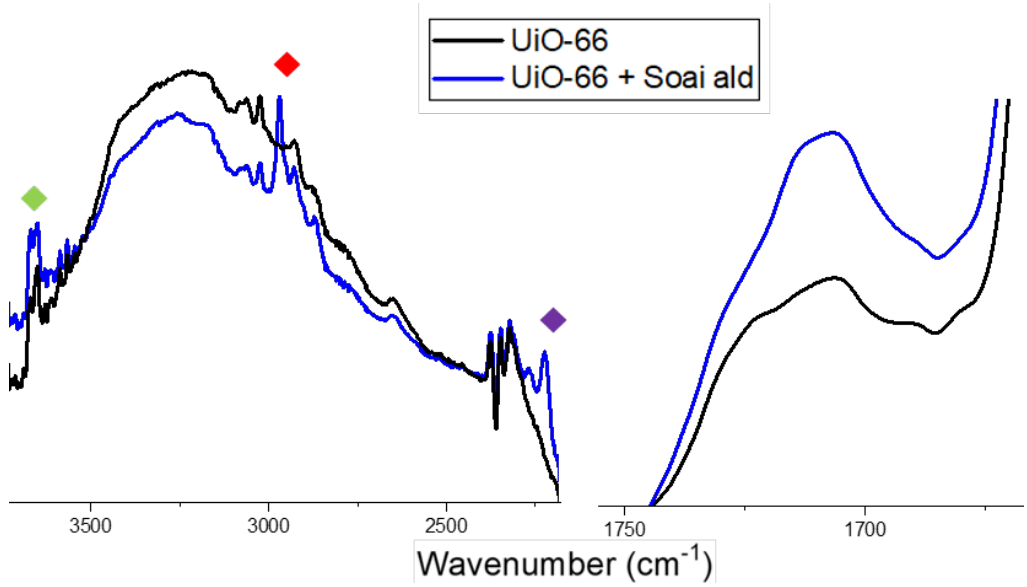

Figure 6. ATR–IR of UiO-66 and UiO-66 after inclusion of aldehyde 1. On the left, stretching of the hydroxyl groups (in green), stretching of the terbutyl/isopropyl groups (in red), stretching of the C-N of the ring (in purple). On the right, stretching of the carbonyl group.

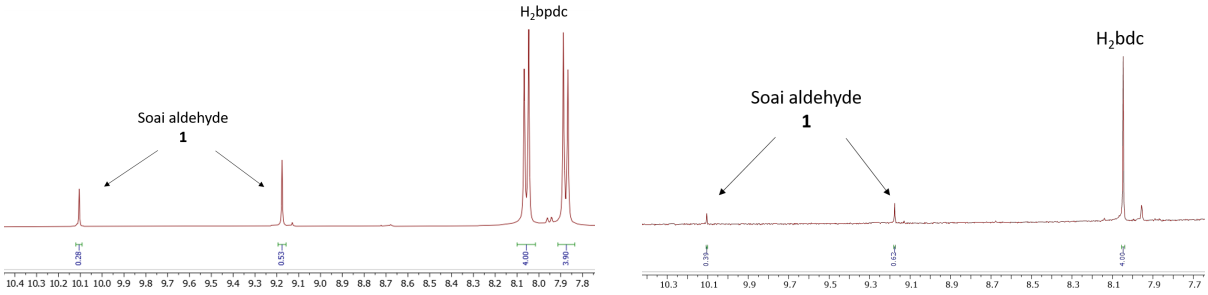

Figure 7. ^{1}H NMR of digested UiO-67 (left) and UiO-66 (right) in acidic solution of 1% D_3PO_4 in DMSO-d_6.

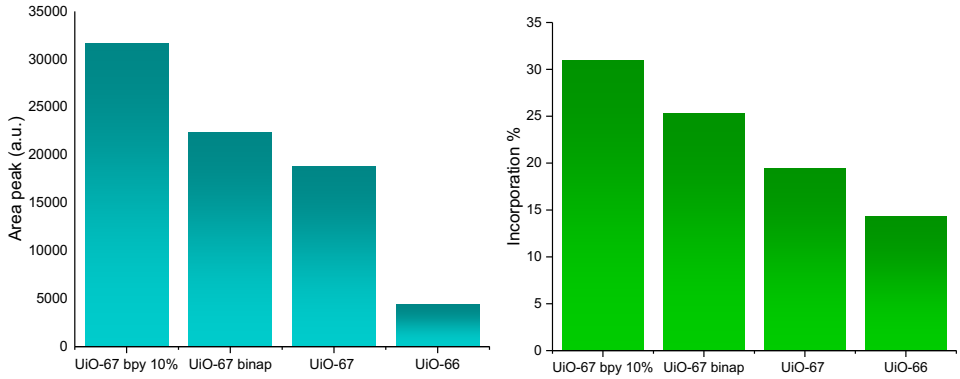

Figure 8. HPLC (left) and NMR (right) quantification of 1 in different UiO MOFs.

Vapour phase reaction set-ups

Recently, we have reported two set-ups to perform vapour-phase reactions [23]. These set-ups have been employed for the experiments described in the next section. In the first set-up, the Soai reagent (pristine **1** or included in the MOFs) is placed on the top of a cylindrical glass support, the support arranged inside a glass vial. In the second setup up to three cylindrical glass supports containing the reagent were located in a bigger vial, in an attempt to secure that the conditions of the gas phase reaction were the same in all the samples. In both cases, Zn(i-Pr)$_2$ solution in toluene is added on the bottom under inert atmosphere and the vial is immediately sealed (See SI, Section 1).

The first set-up has been employed for the experiments of Table 6, while the second set-up for all the other reported experiments.

Results and discussion

(a) Preliminary results

All reactions were conducted at room temperature, and stopped after 24 hours if not specified otherwise, with reaction conditions varying in concentration of substrate, nature and size of the MOF and potentially relevant chiral trigger alkanol **2**.

Firstly, our interest has been focused on the reactivity of the Soai aldehyde **1** in three different materials. We began our studies with a set of gas phase reactions with pristine Soai aldehyde **1,** unwashed UiO-67 with included **1** and washed UiO-67 with included **1** respectively. Under these different conditions, subjecting aldehyde **1** to reaction with iPr_2Zn vapour allowed symmetry breaking by absolute asymmetric alkylation to afford alkanol **2**. This observation was expected for pristine substrate **1**, based on previous literature, although in the present experiment a remarkable 88% *ee* is reached. However, this amplification is affected by the confinement conditions in MOF. In terms of conversion, the washed MOF sample provided a slightly lower conversion compared to the other two samples. In contrast, the final ee% of the unwashed MOF was more similar to the pristine Soai powder, even with an opposite handedness of the product (*S*)-**2** in 70% ee, whereas the washed MOF sample yielded a lower amplification of (*R*)-**2** with 38% ee *(Table 1)*.

The results in *Table 1* are in line with those obtained with the leakage experiments in washed *vs.* unwashed UiO-67. In the unwashed sample the Soai aldehyde **1** is confined in the framework but at the same time an excess of aldehyde **1** is also present on the surface of the MOF. The latter corresponds to surface confinement which reacts in a similar way to the pristine powder of **1**. In contrast, after several washes there is little or no Soai aldehyde present on the surface and the UiO-67 MOF contains only confined **1**. Thus, the conversion of Soai aldehyde **1** into Soai alcohol **2** takes place only within the pores of the MOF.

A second series of experiments has been performed exposing the same substrate, washed UiO-67, but in different scale, to $Zn(i\text{-}Pr)_2$ vapors. The results shown in *Table 2* reveal comparable conversions and final ee% obtained after reaction.

On the basis of these *observations*, it was reasonable to think that instead of the amount of MOF powder with included **1**, the different ratio of **1** in the MOF could play a crucial role in the reaction outcome. However, as shown in in table 3, similar results were obtained in terms of conversion and amplification. UiO-67 with different loadings of included aldehyde **1** have been obtained and tested to the reaction. The amount of aldehyde **1, confined in MOF,** has been evaluated by NMR analysis. Even different amounts of aldehyde **1** in the framework seem to not play a role in the final outcome of the reaction. A possible explanation would be that,

even if the MOFs has different loading of aldehyde **1**, this loading is not significant to make a difference in the reaction outcome. Probably a similar experiment with, for instance, MOFs with 3%, 100% and 300% inclusion of aldehyde **1** would give different results, but the difficulty to reach such high inclusion percentages makes difficult to prove the assumption.

To better understand what could influence the outcome of the reaction in terms of handedness and conversion, a mixture of Soai aldehyde **1** and Soai alcohol **2** has been included in three samples of UiO-67. The initial solution for the inclusion had an aldehyde:alcohol ratio of 1:0,2, but in two out of three samples the ratio of the included species was found lower. The samples have then been tested to vapour phase reaction and the results are shown in Table 4.

The alcohol included was able to direct the handedness of the new formed alcohol, but the amplification of *ee* was seen only in the first case. The amount of alcohol **2** in the framework is lower compared to aldehyde **1**, and it can be speculated that it won't be present in all MOF crystals and all framework cavities. There will be reaction cycles in certain crystals whose outcome in terms of handedness of alcohol **2** will be dictated by the presence of the already included alcohol, and "competing" reaction cycles that will develop under absolute conditions (without alcohol **2**) with a random distribution of enantiomers for the product, The result of this multi-site reaction system, enhanced by the diffusion problems of the reaction intermediates, is that the presence of the reaction catalyst is almost uninfluential.

Tables 1-4. Variations of reaction conditions.

Substrates	Tabel 1 Enantiomer	ee%	Conversion
Soai aldehyde	(R)	88 %	99 %
Unwashed UiO-67	(S)	70 %	98 %
Washed UiO-67	(S)	38 %	82 %

Amount of UiO-67	Table 2 Enantiomer	ee%	Conversion
1,5 mg	(R)	43,50 %	95,50 %
3 mg	(R)	43,50 %	91,50 %
6 mg	(R)	46 %	88 %

Table 3				
UiO-67 sample	**Incorporation (NMR)**	**Enantiomer**	**ee%**	**Conversion**
1	2.5%	(R)	28 %	69 %
2	10.5%	(R)	22,50 %	70 %
3	11 %	(R)	23,50 %	72 %

Table 4			
Initial Alcohol included	**Ratio 1:2**	**Alcohol yielded**	**Conversion**
(R)-**2** 15% ee	1:0.2	(R)-**2** 50% ee	81 %
(S)-**2** 50% ee	1:0.07	(S)-**2** 39% ee	80 %
(R)-**2** 96% ee	1:0.11	(R)-**2** 69% ee	84 %

Table 1: Vapour phase reaction on three different substrates

Table 2: Vapour phase reaction on different amount of washed UiO-67

Table 3: Vapour phase reaction on UiO-67 with different load of **1**

Table 4: Vapour phase reaction on UiO-67 with Soai aldehyde **1** and different Soai alcohols **2**

b) Kinetic plots of the gas phase reactions

Three samples of pristine Soai aldehyde, Soai aldehyde included in UiO-67 and Soai aldehyde included in UiO-66 have been placed in several glass vials, the addition of the $Zn(i\text{-}Pr)_2$ solution has been performed at the same time and the reaction has been stopped at fixed time interval. Conversion and *ee*% obtained in the three different samples have been measured with HPLC and plotted in *Figure 9a* and *Figure 9b*.

These show that after reaction initiates, conversion is more significant in pristine and confined Soai **1** in UiO-67 to reach 80%, while reaction in UiO-66 levels-off at 40% conversion. While symmetry breaking remains a random event, amplification of **2** up to 80% ee is favoured by abundance of starting substrate **1** at the expense of confined reactions, ranging between 34-40% ee.

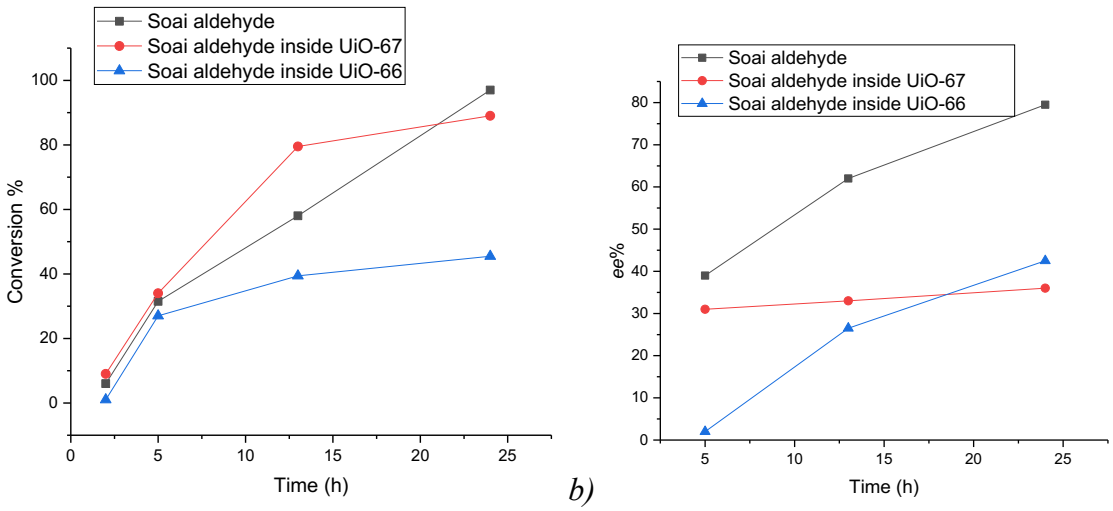

a) *b)*

Figure 9. Kinetic plots of: a) Conversion vs. time; b) ee%% vs. time.

In the same way the kinetic profile of the reaction hav been compared in pristine Soai aldehyde, Soai aldehyde included in UiO-67 and Soai aldehyde included in UiO-67 $bpy_{10\%}$. (*Figure 10a* and *Figure 10b*).

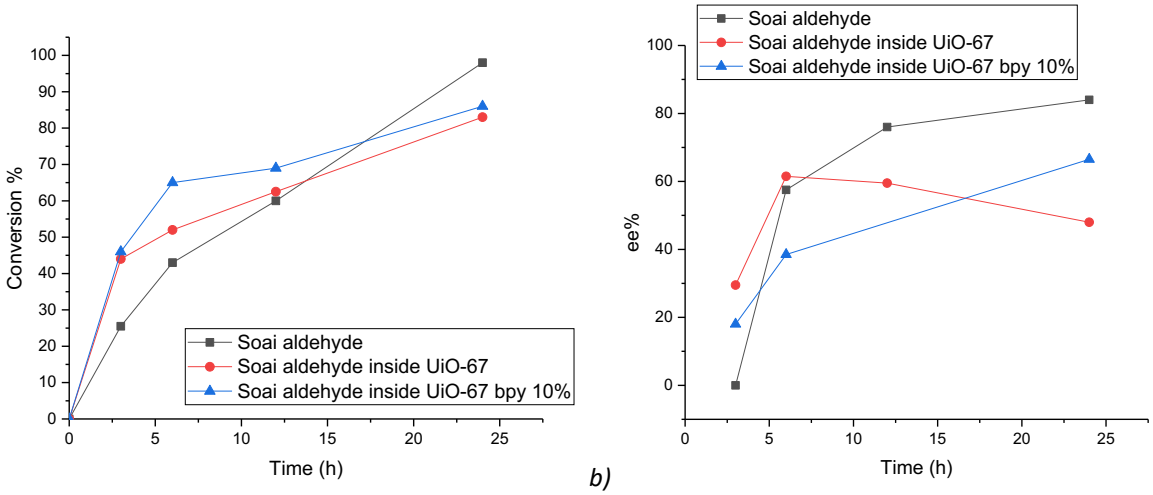

a) *b)*

Figure 10. Kinetic plots of: a) Conversion vs. time; b) ee%% vs.

The kinetic plot of the conversion demonstrates an initial higher rate for the reaction confined in both the UiO-67 in respect to the pristine Soai aldehyde. The observed reactivity may find explanation in the ability to entrap and diffuse vapors of $Zn(i\text{-}Pr)_2$ within the cavities of the MOF. Moreover, introduction of the bipyridine linker in the UiO-67 $bpy_{10\%}$ provides an additional coordination point for the zincorganil reagent, which allows for a controlled diffusion as compared to UiO-67. Even the small cavities of the UiO-66 are able to allocate the oligomers of the catalytic cycle, even if with lower conversions, and the worse results

compared to UiO-67 are easily explainable with the even stronger diffusion problems of reaction intermediates between these cavities.

The enantiomer formed in higher percentage in all the reactions performed was **(R)-2**. The *ee*% was found always lower in the MOFs compared to the pristine aldehyde, a consequence of the limited space available for the reaction to propagate due to the confinement in the framework. Although amplification keeps pace.

c) Screening of different UiO MOFs

To make sure the symmetry breaking in MOFs follows a random event and allows for absolute asymmetric synthesis, we conducted the exposure experiments by using MOFs and $Zn(i\text{-}Pr)_2$ different origins. Thus, a number of inclusion forms of aldehyde **1** were screened to the vapour phase reactions with three different $Zn(i\text{-}Pr)_2$ batches. The zinc solutions were added at the same time and the reactions stopped on every run after 7 days. The results are shown in *Table 6*.

Table 6. Screening of different UiO MOFs to the gas phase reaction.

Soai reagent	Zinc batch 1	Zinc batch 2	Zinc batch 3
Pristine	ee% = 93% conversion = 99%	ee% = 92% conversion = 99%	ee% = 94% conversion = 99%
UiO-67	ee% = 23% conversion = 93%	ee% = 30% conversion = 93%	ee% = 14% conversion = 92%
UiO-67 bpy$_{10\%}$	ee% = 19% conversion = 81%	ee% = 26% conversion = 86%	ee% = 48% conversion = 89%
UiO-67 binaphtyl	ee% = 21% conversion = 80%	ee% = 43,5% conversion = 72%	ee% = 28% conversion = 82%
UiO-66	ee% = 32% conversion = 55%	ee% = 35% conversion = 51%	ee% = 16% conversion = 43%

Legend: (R)-enantiomer / (S) – enantiomer obtained in higher percentage

In absence of chiral inductor, alkylation of aldehyde **1** in UiO MOFs provide enantiomers of the alcohol **2** at random, a characteristic feature of an Absolute Asymmetric Synthesis. The low amplification level of *ee* in MOFs compared to the pristine Soai aldehyde can be explained

by the confinement effect of the framework of the MOF: this constraint results in limited diffusion of the oligomeric species involved in the autocatalytic cycles. Thus, autocatalysis is probably confined to several reaction compartments, and the final *ee*% consists of a sum of the total autocatalytic cycles occurring in multiple local sites of the MOF. In contrast, in the pristine Soai all the aldehyde molecules are part of a continuum allowing for a same autocatalytic cycle. The rising *ee*% may be reflecting the local chirality in UiO series. Considering the 15 reactions performed in *Table 6*, five of them yielded **(S)-2**, while the other ten yielded **(R)-2**. This could reflect a *pro*-R orientation of the Soai aldehyde in the pristine state and included in the MOF.

d) Analyses on the materials after the vapour-phase reactions

Two samples of pristine UiO-67 $bpy_{10\%}$ and UiO-67 $bpy_{10\%}$ with included aldehyde **1** were subjected to the vapour phase reaction. *Figure 12* depicts the Capillary X-ray diffraction (C-XRD) pattern of both the material which resembles the C-XRD of pristine MOF. This shows that both materials maintain crystallinity after reaction. The Zr cluster ($Zr_6O_6(bpdc)_6$) contains μ_3-OH. This site may provide an additional anchoring point for $Zn(iPr)_2$ during the vapour phase reaction (*Figure 11*).[24] Closer analyses at the XRD diffractograms did not show any interaction between zinc reagents and the clusters. Moreover, Soai has shown that the presence of additives containing hydroxyl moieties does not interfere with the autocatalytic process and the asymmetric amplification [25].

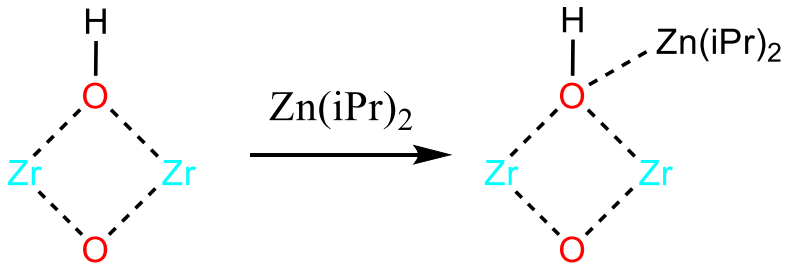

Figure 11. Possible interaction between $Zn(i\text{-}Pr)_2$ and the Zr-O moiety of the MOF cluster.

ATR-IR analysis has also been carried out on the MOF samples after reaction. Confronting the spectra of the three materials in *Figure 13*, the C=O stretching of the carbonyl group of aldehyde **1** at 1700 cm^{-1}, (totally absent in the parent material), almost disappears in the UiO-67 after vapour phase reaction. Although diagnostic signals of the alcohol group of **2** are not possible to detect (hidden by peaks of the carboxylate linkers), other signals, common to both **1** and **2** are visible: the C-H stretching of the terbutyl/isopropyl groups below 3000 cm^{-1} and the C-N stretching of the ring at 2200 cm^{-1}. The stretching of the O-H groups above 3500 cm^{-}

[1], present in the pristine material and perturbed in the material after the inclusion, is still perturbed after the vapour phase reaction. This hints that alcohol **2** is still allocated on the cluster. The ATR-IR analysis alone indicates that a similar molecule to aldehyde **1** is present in the material, and they complement nicely the results obtained through other techniques and described above

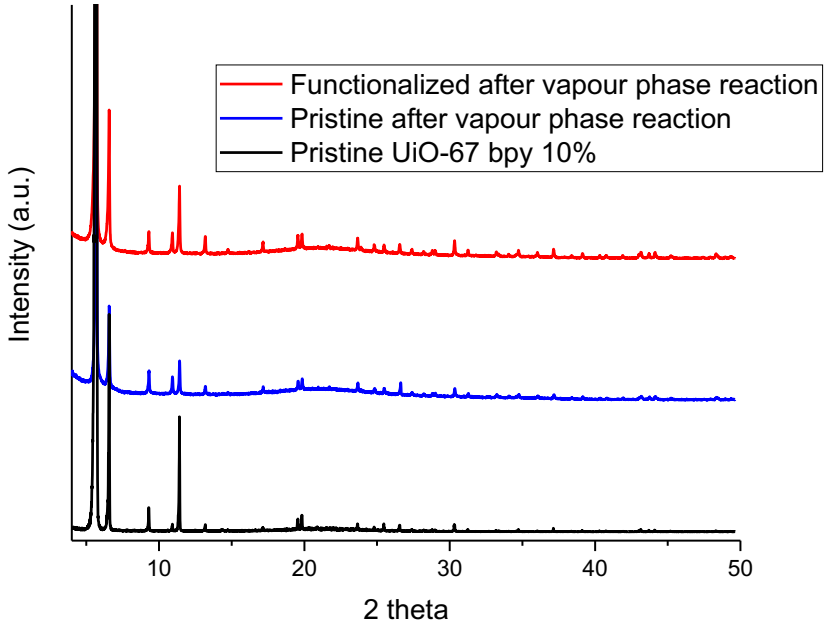

Figure 12. XRD analysis on the MOFs.

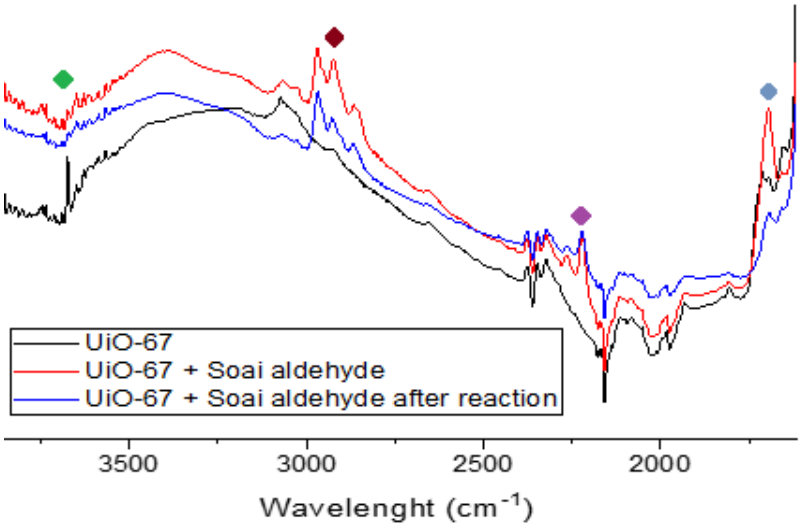

Figure 13. IR analysis on the UiO-67 after vapour phase reaction. Stretching of the hydroxyl groups (in green), stretching of the terbutyl group (in red), stretching of the C-N of the ring (in purple), stretching of the carbonyl group (in blue).

Conclusions

In summary, we have demonstrated that symmetry breaking in conjunction with autocatalytic amplification is realizable in confined environment. Thus, under heterogenous conditions and in absence of chiral polarization, absolute asymmetric synthesis of alkanol **2** by reaction of $Zn(iPr)_2$ vapor with aldehyde **1** confined in UiO-MOF series.

The results show a somehow faster reaction in the MOFs than in the pristine materials, and that confinement in different frameworks can contribute to the final conversion. Moreover, moderate amplification of *ee* were found reactions in UiO-MOFs as confinement leads to limited diffusion and propagation of chiral active Zn-**2**. We postulate that amplification of alkanol **2** is initiated by nucleation at different site in the MOF. Generally, stochastic formation of (*S*)- and (*R*)-**2** is observed, therefore it is conceivable that this also the case within the MOF. These nucleations taking place with opposite configurations at different sites accounts for the low amplification, which is summed up in the final measured *ee*. ATR-IR data localize aldehyde **1** in close proximity to the Zr-cluster, in agreement with DFT calculations, which also the case for product **2** after reaction. Also, the crystallinity of the MOF is well preserved after vapour phase reaction with $Zn(iPr)_2$. To our knowledge this is the first example of symmetry breaking for autocatalytic amplification in confined environment.

References

[1] a) K. Mislow, *Collect. Czech. Chem. Commun.* **2003**, *68*, 849-864; b) M. Bolli, R. Micura and A. Eschenmoser, *Chemistry & Biology* **1997**, *4*, 309-320; c) B. L. Feringa and R. A. van Delden, *Angewandte Chemie-International Edition* **1999**, *38*, 3419-3438; d) S. Pizzarello and A. L. Weber, *Science (Washington, DC, U. S.)* **2004**, *303*, 1151; e) I. Weissbuch and M. Lahav, *Chem. Rev. (Washington, DC, U. S.)* **2011**, *111*, 3236-3267; f) J. S. Siegel, *Chirality* **1998**, *10*, 24-27; g) J. M. Ribo, C. Blanco, J. Crusats, Z. El-Hachemi, D. Hochberg and A. Moyano, *Chem. - Eur. J.* **2014**, *20*, 17250-17271.

[2] a) A. J. Bissette and S. P. Fletcher, *Angew. Chem., Int. Ed.* **2013**, *52*, 12800-12826; b) D. G. Blackmond, *Chemical Reviews* **2020**, *120*, 4831-4847.

[3] F. C. Frank, *Biochimica et Biophysica Acta* **1953**, *11*, 459-463.

[4] K. Soai, T. Shibata, H. Morioka and K. Choji, *Nature* **1995**, *378*, 767-768.

[5] a) I. Sato, H. Urabe, S. Ishiguro, T. Shibata and K. Soai, *Angewandte Chemie International Edition* **2003**, *42*, 315-317; b) T. Shibata, S. Yonekubo and K. Soai, *Angewandte Chemie International Edition* **1999**, *38*, 659-661.

[6] a) K. Soai, T. Kawasaki and A. Matsumoto, *Accounts of Chemical Research* **2014**, *47*, 3643-3654; b) K. Soai, T. Kawasaki and A. Matsumoto, *Tetrahedron* **2018**, *74*, 1973-1990.

[7] a) D. A. Singleton and L. K. Vo, *Organic Letters* **2003**, *5*, 4337-4339; b) K. Soai, I. Sato, T. Shibata, S. Komiya, M. Hayashi, Y. Matsueda, H. Imamura, T. Hayase, H. Morioka, H. Tabira, J. Yamamoto and Y. Kowata, *Tetrahedron: Asymmetry* **2003**, *14*, 185-188.

[8] Y. Kaimori, Y. Hiyoshi, T. Kawasaki, A. Matsumoto and K. Soai, *Chemical Communications* **2019**, *55*, 5223-5226.

[9] G. Rotunno, D. Petersen, M. Amedjkouh, ChemSystemsChem 2020, 2, DOI: 10.1002/syst.201900060

[10] a) B. L. Feringa and R. A. van Delden, *Angewandte Chemie International Edition* **1999**, *38*, 3418-3438; b) K. Mislow, *Collect Czech Chem Commun.* **2003**, *68*, 849.

[11] a) D. G. Blackmond, C. R. McMillan, S. Ramdeehul, A. Schorm and J. M. Brown, *Journal of the American Chemical Society* **2001**, *123*, 10103-10104; b) F. G. Buono and D. G. Blackmond, *Journal of the American Chemical Society* **2003**, *125*, 8978-8979.

[12] a) I. D. Gridnev, J. M. Serafimov and J. M. Brown, *Angewandte Chemie International Edition* **2004**, *43*, 4884-4887; b) I. D. Gridnev and J. M. Brown, *Proceedings of the National Academy of Sciences of the United States of America* **2004**, *101*, 5727; c) J. Klankermayer, I. D. Gridnev and J. M. Brown, *Chemical Communications* **2007**, 3151-3153; d) I. D. Gridnev, J. M. Serafimov, H. Quiney and J. M. Brown, *Organic & Biomolecular Chemistry* **2003**, *1*, 3811-3819.
[13] M. E. Noble-Terán, J.-M. Cruz, J.-C. Micheau and T. Buhse, *ChemCatChem* **2018**, *10*, 642-648.
[14] I. D. Gridnev and A. K. Vorobiev, *ACS Catalysis* **2012**, *2*, 2137-2149.
[15] a) L. Schiaffino and G. Ercolani, *Angewandte Chemie International Edition* **2008**, *47*, 6832-6835; b) L. Schiaffino and G. Ercolani, *Chemistry* **2010**, *16*, 3147-3156; c) G. Ercolani and L. Schiaffino, *J Org Chem* **2011**, *76*, 2619-2626.
[16] A. Matsumoto, T. Abe, A. Hara, T. Tobita, T. Sasagawa, T. Kawasaki and K. Soai, *Angewandte Chemie International Edition* **2015**, *54*, 15218-15221.
[17] a) E. Doka and G. Lente, *J. Am. Chem. Soc.* **2011**, *133*, 17878-17881; b) O. Fulop and B. Barabas, *J. Math. Chem.* **2016**, *54*, 10-17; c) B. Barabas, R. Kurdi, C. Zucchi and G. Palyi, *Chirality* **2018**, *30*, 913-922; d) B. Barabas, J. Toth and G. Palyi, *J. Math. Chem.* **2010**, *48*, 457-489; e) D. G. Blackmond, *Tetrahedron: Asymmetry* **2006**, *17*, 584-589; f) J.-C. Micheau, C. Coudret, J.-M. Cruz and T. Buhse, *Physical Chemistry Chemical Physics* **2012**, *14*, 13239-13248.
[18] S. V. Athavale, A. Simon, K. N. Houk and S. E. Denmark, *Nature Chemistry* **2020**, *12*, 412-423.
[19] Y. Kaimori, Y. Hiyoshi, T. Kawasaki, A. Matsumoto and K. Soai, *Chemical Communications* **2019**, *55*, 5223-5226.
[20] R. Batten Stuart, R. Champness Neil, X.-M. Chen, J. Garcia-Martinez, S. Kitagawa, L. Öhrström, M. O'Keeffe, M. Paik Suh and J. Reedijk in *Terminology of metal–organic frameworks and coordination polymers (IUPAC Recommendations 2013)*, *Vol. 85* **2013**, p. 1715.
[21] a) A. Gheorghe, M. A. Tepaske and S. Tanase, *Inorganic Chemistry Frontiers* **2018**, *5*, 1512-1523; b) X. Li, J. Wu, C. He, Q. Meng and C. Duan, *Small* **2019**, *15*, 1804770; c) S. Bhattacharjee, I. M. Khan, X. Li, Q.-L. Zhu and X.-T. Wu, *Catalysts* **2018**, *8*; d) A. V. Artem'ev and V. P. Fedin, *Russian Journal of Organic Chemistry* **2019**, *55*, 800-817.
[22] J. H. Cavka, S. Jakobsen, U. Olsbye, N. Guillou, C. Lamberti, S. Bordiga and K. P. Lillerud, *Journal of the American Chemical Society* **2008**, *130*, 13850-13851.
[23] G. Rotunno, D. Petersen and M. Amedjkouh, *ChemSystemsChem* **2020**.
[24] a) L. C. Gallington, I. S. Kim, W.-G. Liu, A. A. Yakovenko, A. E. Platero-Prats, Z. Li, T. C. Wang, J. T. Hupp, O. K. Farha, D. G. Truhlar, A. B. F. Martinson and K. W. Chapman, *Journal of the American Chemical Society* **2016**, *138*, 13513-13516; b) I. S. Kim, J. Borycz, A. E. Platero-Prats, S. Tussupbayev, T. C. Wang, O. K. Farha, J. T. Hupp, L. Gagliardi, K. W. Chapman, C. J. Cramer and A. B. F. Martinson, *Chemistry of Materials* **2015**, *27*, 4772-4778.
[25] a) T. Kawasaki, Y. Wakushima, M. Asahina, K. Shiozawa, T. Kinoshita, F. Lutz and K. Soai, *Chemical Communications* **2011**, *47*, 5277-5279; b) T. Shibata, H. Tarumi, T. Kawasaki and K. Soai, *Tetrahedron: Asymmetry* **2012**, *23*, 1023-1027.